Polarizing properties and structural characteristics of the cuticle of the scarab Beetle *Chrysina gloriosa* ☆

CrossMark

Lía Fernández del Río *, Hans Arwin, Kenneth Järrendahl

Laboratory of Applied Optics, Department of Physics, Chemistry and Biology, Linköping University, SE-581 83 Linköping, Sweden

ARTICLE INFO

ABSTRACT

The scarab beetle *Chrysina gloriosa* is green with gold-colored stripes along its elytras. The properties of light reflected on these areas are investigated using Mueller-matrix spectroscopic ellipsometry. Both areas reflect light with high degree of left-handed polarization but this effect occurs for specular reflection for the gold-colored areas and for off-specular angles for the green areas. The colors and polarization phenomena originate from reflection of light in the cuticle and a structural analysis is presented to facilitate understanding of the different behaviors of these two areas. Scanning electron microscopy (SEM) images of the cross section of beetle cuticles show a multilayered structure. On the gold-colored areas the layers are parallel to the surface whereas on the green-colored areas they form cusp-like structures. Optical microscopy images show a rather flat surface in the gold-colored areas compared to the green-colored areas which display a net of polygonal cells with star-shaped cavities in the center. Each of the polygons corresponds to one of the cusps observed in the SEM images. Atomic force microscopy images of the star-shaped cavities are also provided. The roughness of the surface and the cusp-like structure of the green-colored areas are considered to cause scattering on this area.

1. Introduction

Chrysina beetles are also known as jewel scarabs because of their brilliant iridescence and metallic coloration which make them highly priced by insect collectors. They can be found from southern USA to Central America in pine, juniper and pine-oak forests where they are easily camouflaged [1].

The attractive shiny metallic colors of these scarab beetles have also made them the focus of several scientific investigations. The colors are mainly structural and originate from reflection of light in the cuticle [2]. Back in the early 1900s Michelson noticed that the jewel scarab *Plusiotis* (now *Chrysina*) *resplendens* reflects circularly polarized light [3] which later led to a series of investigations on the polarization properties of several scarab beetles [4,5].

In nature the appearance of polarized light is common and several animals use linearly polarized light for orientation and navigation. Some animals have developed structures in their bodies which reflect polarized light, in some cases near-circular [6]. The fact that some animals are able to reflect polarized light suggests that they are able to detect it and use it to communicate or as a defense mechanism [7]. The ability to detect circularly polarized light has also been investigated

for *Chrysina gloriosa* (*C. gloriosa*) LeConte 1854 [8] and for *Anomala dubia*, *Anomala vitis*, *Cetonia aurata* and *Potosia cuprea* [9] as well as for some other animals [10].

The invention of the electron microscope in the mid 1900s made it possible to study microstructures including the structural composition of insect cuticles. In many cases the cuticle consists of planes of microfibrils which may either form preferred oriented layers or rotate progressively to form helicoidal structures [11] known as Bouligand structures [12]. A cusp-like structure of concentric layers that matches polygonal cells on the surface has also been identified in *C. gloriosa* [13] and other beetles from the same family [14].

More recently, an effort to understand the helicoidal structure and its influence on the polarization of light has lead to the creation of models that reproduce this structure and its optical response. Layered biaxial materials with a continuous rotation as well as twisted lamellar structures have already been characterized [15–19].

A combination of polarization measurements and imaging to characterize the localization of circular polarization on beetle cuticles is also of interest and it is now possible with the development of an angle resolved Mueller-matrix polarimeter [20].

Most investigations carried out so far share the goal of determining the structure and composition of beetle cuticles and understanding the polarization of light reflected on them. A future objective is to develop artificial bioinspired multilayer systems which reproduce the optical effects of beetles' exoskeletons [21,22].

In this paper we report an investigation of the optical properties in terms of spectral, polarization and scattering features of the exoskeleton

---

* Corresponding author.
E-mail address: liafe@ifm.liu.se (L. Fernández del Río).

of the scarab beetle *C. gloriosa* and relate these properties to established knowledge about its structure. This beetle polarizes light right- and left-handed near-circular but in a different way on different parts of its exoskeleton [23].

2. Experimental details

The specimens of *C. gloriosa* used in this work were collected at the Nature Conservancy in the Texas Davis Mountains and was kindly provided by P. Brady at the University of Texas at Austin. We used several techniques to analyze the optical properties and the structure of the exoskeleton of *C. gloriosa*. The analyzed areas were the elytras (the wing covers) which are green-colored but with gold-colored stripes along them (Fig. 1).

The cuticle is composed of proteins, lipids and chitin and is divided into epicuticle, exocuticle and endocuticle [2]. The outermost layer, the epicuticle, is a very thin layer mainly composed of proteins, lipids, lipoproteins and dihidroxyphenols and covered by wax and cement. The exocuticle is a dense layer composed of protein, chitin crystallites and low concentrations of liquid. In some cases it is divided into an outer- and an inner-exocuticle which at the same time are divided into sub-layers. Underneath it is the endocuticle, with a higher liquid concentration.

After an initial test with a left-circular and a right-circular polarizing filter a detailed analysis of the reflected light was performed using Mueller-matrix spectroscopic ellipsometry (MMSE). The instrument used for this investigation (RC2, J. A. Woollam Co., Inc.) has dual rotating compensators making it possible to obtain the complete normalized Mueller-matrix.

Measurements are performed in the spectral range 245–1690 nm at multiple angles of incidence. The use of focusing lenses limited the spectral range to 245–1000 nm but allowed us to measure in a smaller area with approximately a width of 50 μm and a length of 50–200 μm depending on angle of incidence.

Two different types of measurements were performed. First, specular MMSE measurements were performed at incident angles from 20° to 75° in steps of 5° where the angular limits were determined by the focusing optics and the beam size. A step of 5° gave a good angular overview of the changes with angle of incidence. Between each measurement the sample was realigned at each angle. An acquisition time of 30 s was found sufficient to achieve a good signal-to-noise ratio.

In the second type of measurement scattered light was investigated. In this case, the sample holder was fixed at an incident angle of 45°. Data acquisition was then performed by moving the detector ±15° off the specular direction in steps of 3°, that is, the detector angles ranged from 30° to 60°. The acquisition time was increased to 60 s due to the lower intensity of the scattered light.

The results will be presented as polar contour plots where different parameters are represented as a function of angle of incidence θ and wavelength λ of the incident beam. The parameters presented are the m_{41}-element of the Mueller-matrix, the degree of polarization P of the reflected light, the ellipticity e and the absolute value of the azimuth angle α of the polarization ellipse. Values for P, e and α are determined for incident light with normalized Stokes vector $\mathbf{S}_i = [1,0,0,0]^T$. With normalized Mueller matrices ($m_{11} = 1$), the polarization state of the reflected light will be $\mathbf{S}_0 = [1,m_{21},m_{31},m_{41}]^T$. Thus, m_{41} can be interpreted as the degree of circular polarization of the reflected light in this case.

In the polar plots the radial coordinate is the wavelength λ ϵ [245, 1000] nm, and the angular coordinate is the angle of incidence θ ϵ [20, 75]. In most of the plots the scales represent the complete range of the parameters. The Mueller-matrix elements are normalized and therefore m_{41} ranges from −1 to +1. In some plots the m_{41}-scale is modified to range from minimum and maximum values to enhance visibility of small features. The degree of polarization ranges from 0 (not polarized), to 1 (completely polarized). The ellipticity has values from −1 (left-handed circular polarization) to +1 (right-handed circular polarization). Finally, the absolute value of the azimuth angle is in the range of 0–90°, which in cases when |e| < 1 represents an ellipse with its major axis horizontally orientated (p-polarized) when $\alpha = 0°$, to vertically orientated (s-polarized) when $\alpha = 90°$. The scattering plots show the m_{41}-element of the Mueller-matrix and P in the same wavelength range as determined before.

The surface of the gold- and green-colored areas was imaged with an optical microscope using 100× magnification.

Cross section images of the cuticle were taken with a scanning electron microscope (SEM). The SEM used was a Leo 1550 with a Gemini field emission column. The samples were cooled in liquid nitrogen for 10 min, cut with a razor blade and glued to the sample holder with silver glue. Since the samples are non-conducting a platinum coating was applied during 20 s at 60 mA at a pressure of $5 \cdot 10^{-2}$ Pa. The accelerating voltage was 2 kV.

The surface topography was imaged by atomic force microscopy (AFM). The instrument used was a Dimension 3100 SPM from Veeco Instruments Inc. operated in tapping mode. The scanned areas were 5×5 μm^2 for the gold-colored areas and 10×10 μm^2 for the green-colored areas, with a lateral resolution of about 10 nm.

3. Results

3.1. Polarizing filters

Light reflected from the cuticle of *C. gloriosa* has a high degree of circular polarization. This effect is easily observed through circular polarizers. Fig. 1 shows three pictures of *C. gloriosa* taken with a left-circular polarizer in front of the camera, without polarizer and with a right-circular polarizer in front of the camera.

The figure indicates that *C. gloriosa* reflects left-handed near-circular polarized light and that this effect is similar for the gold- and green-colored areas. However, right-handed polarization effects cannot be excluded based on a simple visual inspection and a detailed MMSE analysis is needed to get a better view of the polarization behavior.

3.2. Mueller-matrix spectroscopic ellipsometry

Fig. 2 shows MMSE results of measurements on the gold-colored areas. The m_{41} plot clearly shows both right- and left-handed polarizations depending on angle of incidence and wavelength. Left-handed polarization can be found at angles from 20° up to 75° and wavelengths from 400 to 700 nm approximately, whereas right-handed polarization is found in a smaller range of angles, from 55° to 75° and wavelengths from 550 to 650 nm. That is, the degree of circular polarization can be very pronounced in the gold-colored areas of the exoskeleton. This is confirmed by the ellipticity plot where both high negative and positive ellipticities are reached.
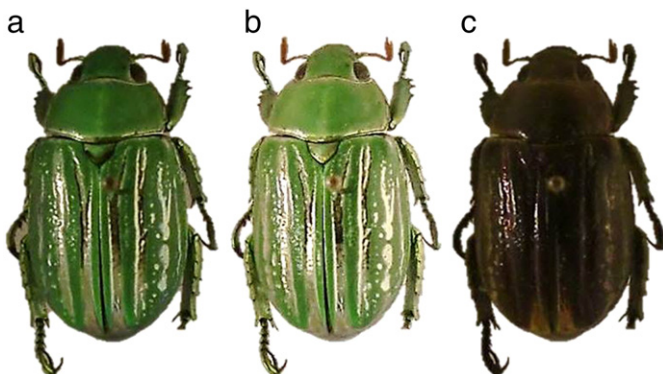

Fig. 1. Images of *C. gloriosa* taken with a left-circular polarizer (LCP) in front of the camera (a), without polarizer (b) and with a right-circular polarizer (RCP) in front of the camera (c).
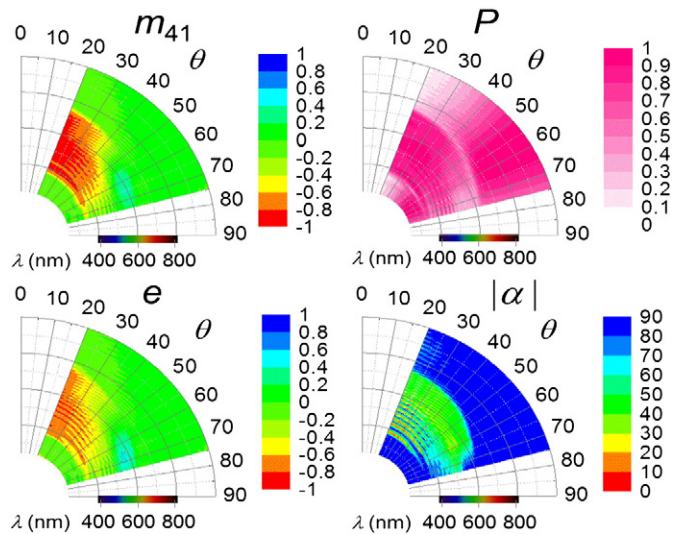
Fig. 2. Contour plots (λ, θ) of the gold-colored area showing the Mueller-matrix element m_{41}, degree of polarization P, ellipticity e and azimuth $|\alpha|$, with $\lambda \in$ [245, 1000] nm and $\theta \in$ [20°, 75°].

Fig. 3a shows the result of the measurements on green-colored areas. These measurements display quite different results. It is observed that even though clear polarization effects are appreciated by eye, the specular MMSE measurements from the green areas show a very low degree of circular polarization and ellipticity. In Fig. 3b m_{41} and the ellipticity are plotted on a min to max scale (from 0.01 to −0.04 and from 0.03 to −0.1, respectively). With this scale it is possible to observe some variation in the data indicating both left- and right-polarizations but the effects are very small.

3.3. Scattering

Fig. 4 shows scattering measurement on a gold-colored area. In this case, left-handed polarization is observed not only for specular reflection but also for scattering at angles spanning over more than ±5°.
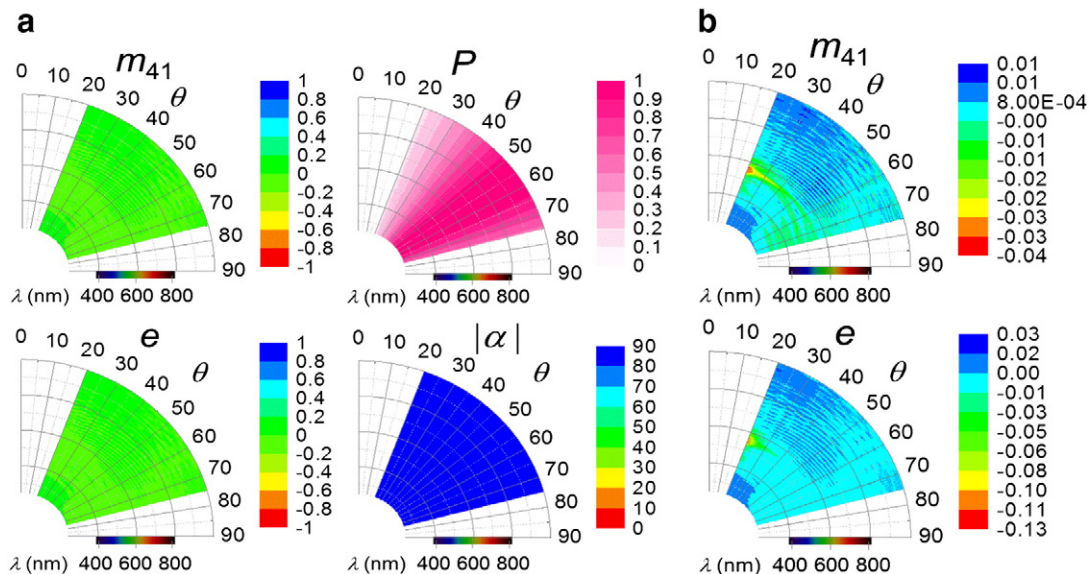

Fig. 4. Contour plots (λ, θ) of the scattering measurements on a gold-colored area showing the Mueller-matrix element m_{41} and the degree of polarization P with $\lambda \in$ [245, 1000] nm and $\theta \in$ [20°, 75°].

The degree of polarization is high at lower scattering angles but decreases considerably for angles larger than ±10°.

The scattering measurements done on a green-colored area are shown in Fig. 5. In contrast to the specular measurements a very clear left-handed polarization at scattering angles from −5° to −15° is observed. In the same region the degree of polarization is close to 1.

3.4. Scanning electron microscopy

The SEM images in Fig. 6a and b show that the exocuticle has two regions. The outer exocuticle found just below the epicuticle has, for this specimen, a thickness of 10 μm and the underlaying inner exocuticle has a thickness of around 6 μm. Both regions are composed of sub-layers with thicknesses of around 200 and 350 nm, respectively.

Fig. 6a shows a cross section of the cuticle from a gold-colored area. We can observe that the sub-layers of the outer and inner exocuticle are parallel to the surface of the exoskeleton. Fig. 6b shows a cross section of the cuticle from a green-colored area. We can identify curved concentric sub-layers with a cusp-like geometry in the outer exocuticle with a column width around 10 μm. The sub-layers in the inner-exocuticle are parallel to the surface.

A surface image of the green-colored area (Fig. 6c) shows a non-flat surface with a starry pattern. The diameter of each star-like cell is approximately 10 μm which is the same as the width of the cusps observed in the cross section suggesting that the center of the cusp corresponds to the center of each star.

Fig. 3. Contour plots (λ, θ) of the green-colored area showing the Mueller-matrix element m_{41}, degree of polarization P, ellipticity e and azimuth $|\alpha|$, with $\lambda \in$ [245, 1000] nm and $\lambda \in$ [20°, 75°]. (a) Using full scale. (b) The m_{41} and ellipticity plots rescaled to maximum and minimum values.
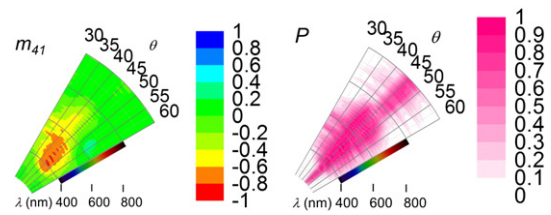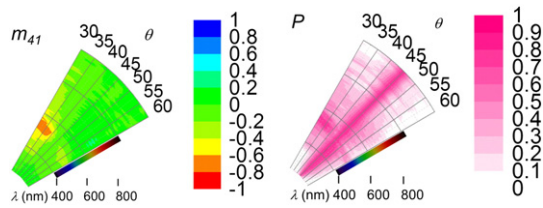
Fig. 5. Contour plots (λ, θ) of the scattering measurements on a green-colored area showing the Mueller-matrix element m_{41} and the degree of polarization P with $\lambda \in [245, 1000]$ nm and $\theta \in [20°, 75°]$.

3.5. Optical microscope

Observations with an optical microscope of the surface of the gold-colored area in Fig. 7a reveal a flat surface whereas the green-colored area in Fig. 7b shows a pattern composed by pentagonal, hexagonal and heptagonal cells. As can be observed from Fig. 7b, each cell has an approximate size of 10 μm and the reflections are bright yellow from the center and greenish from the edges.

3.6. Atomic force microscopy

An AFM image of one of the cells gives us a better understanding of the cusp-like structures. Fig. 8a shows a very flat surface of the gold-colored area and Fig. 8b the star-shaped groove with a depth of 300 nm and an area of 10×10 μm².

4. Discussion

Light reflected from *C. gloriosa* is right- or left-handed polarized depending on the incident angle and wavelength. This effect is easily observed with right- and left-handed polarizers although it is not always obvious when analyzing specularly reflected light with MMSE. The gold-colored areas showed very pronounced polarization effects and have m_{41} values close to -1, that is, at certain angles and wavelengths the reflected light is left-handed and near-circular. Right-handed polarized light is detected but in more limited angle spans and wavelength regions. This effect is also less pronounced. On the green-colored areas the situation is very different. In specular measurements the effect is hard to detect due to the low m_{41} values.

An important fact has been shown here. With simple polarizers it is possible to observe left-handed polarization in both the gold- and the green-colored areas. However, the MMSE analysis shows that the effect for specular reflection is extremely small on the green-colored areas. This suggests that the green-colored areas scatter light whereas the gold-colored areas are good specular reflectors.

To show this, scattering measurements were conducted. The specular reflected light on the gold-colored areas of the beetle is left-handed near-circular polarized at wavelengths from 350 to 550 nm approximately.

On the other hand a different behavior is observed on the green-colored areas which proves to scatter light over a wider angle range. The specularly reflected light is slightly polarized but this effect increases greatly when increasing the scattering angle at wavelengths from 500 to 600 nm. The reflected light is also right-handed polarized at scattering angles from 55° to 60° and for wavelengths from 600 to 700 nm.

Although the gold- and green-colored areas are found mixed in the elytras they must have different structures to generate different colors and polarizing properties. The SEM images show multilayer structures in both areas. The inner exocuticle seems to have a similar structure with the sub-layers parallel to the surface and similar dimensions. However the outer exocuticles have different structures. On the gold-colored areas the exocuticle structure is a stack of sub-
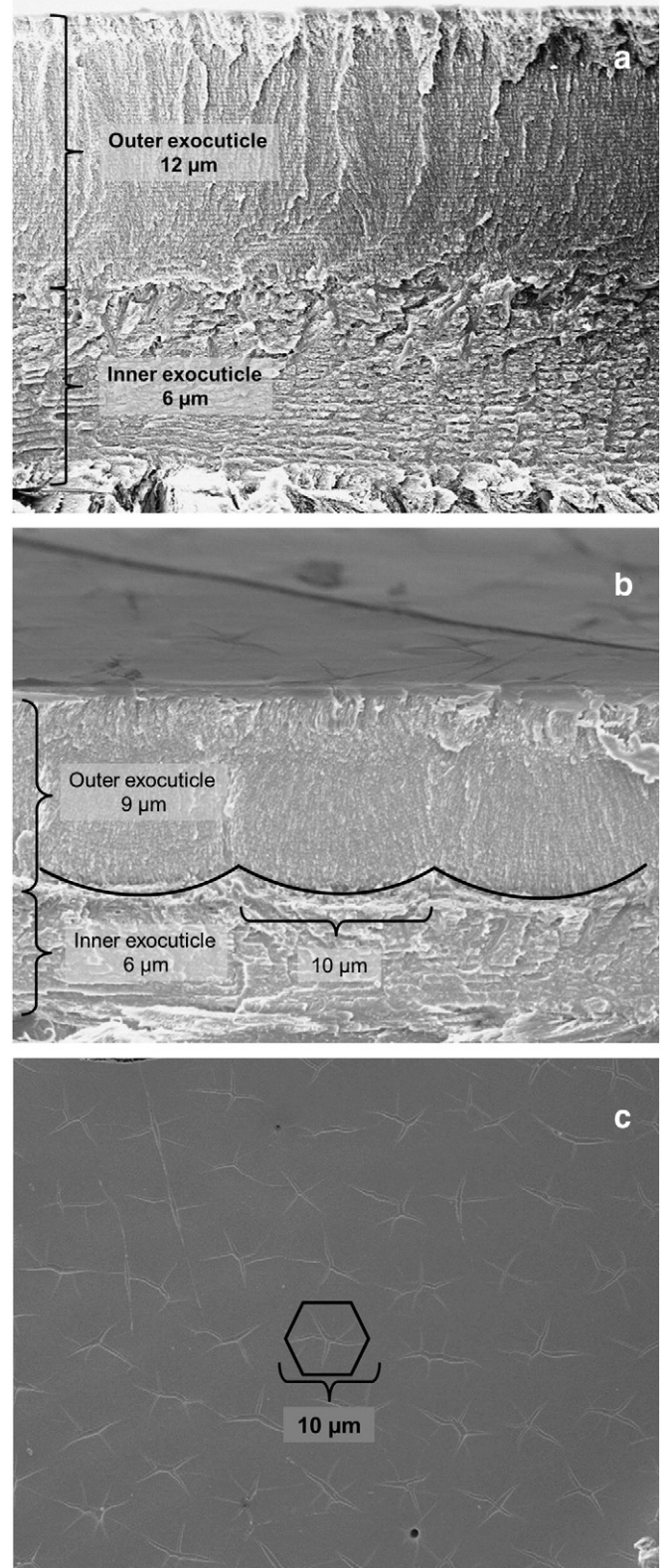

Fig. 6. SEM images showing cross-sections of the cuticle with the surface of the cuticle located at the top of the image, (a) from the gold-colored area and (b) from the green-colored area. (c) SEM image from the surface of the green area showing a starred pattern.

layers parallel to the surface whereas on the green-colored areas the sub-layers have a cusp-like geometry. The average width of the cusps is 10 μm and generates a star-shaped depression on the surface. This pattern is only observed on the SEM images of the green-colored surfaces.
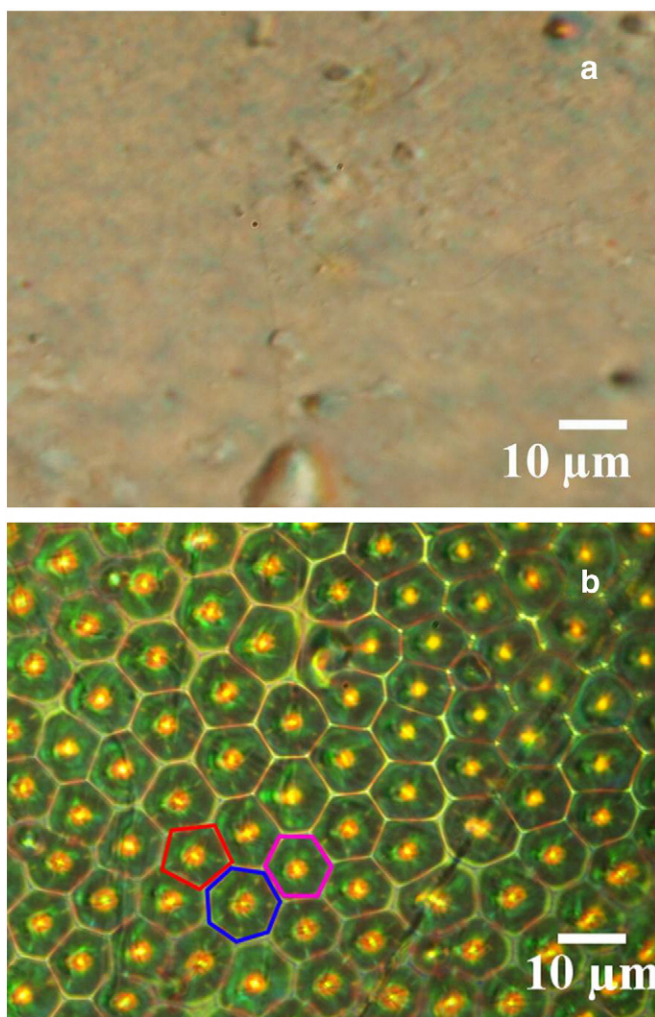
Fig. 7. Optical microscopy image of the surface of (a) a gold-colored area and (b) a green-colored area of the cuticle showing bright yellow reflections from the core of each cell and greenish reflection from the edges. The shape of the cells is pentagonal, represented in red, hexagonal, in pink, and heptagonal, in blue.
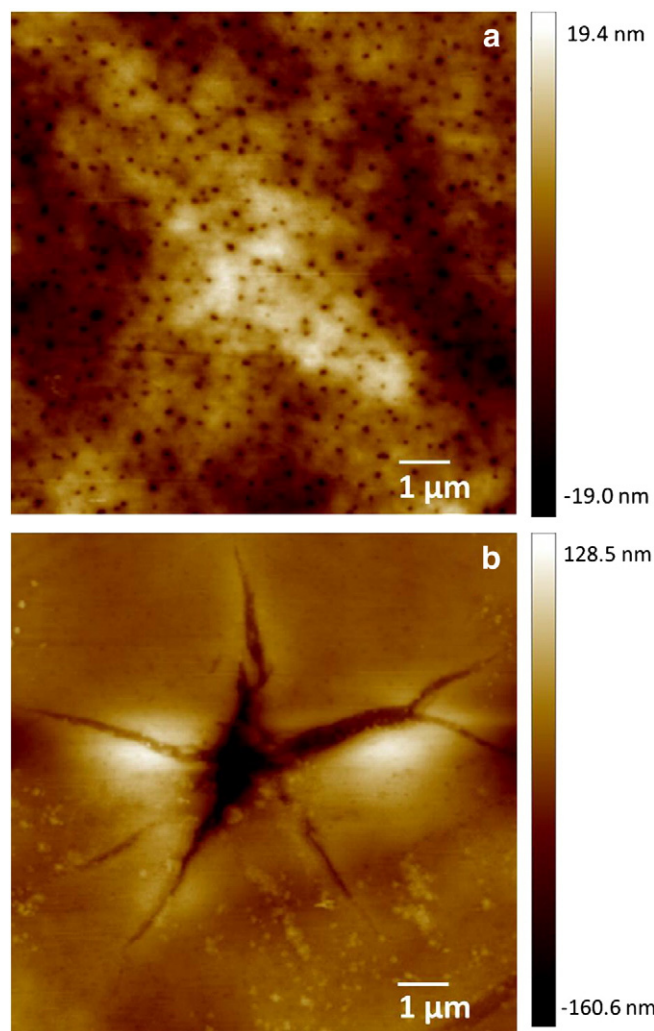

Fig. 8. AFM images of the surfaces of the (a) gold-colored area with 5×5 μm^2 size and (b) green-colored area showing a star-shaped groove with 300 nm depth and 10×10 μm^2 size.

Optical microscopy images of the gold-colored areas show a very flat and uniform surface whereas the green-colored areas are composed of polygonal cells. The cells have pentagonal, hexagonal or heptagonal shape, depending on the curvature of the surface. The diameter is around 10 μm and corresponds to stated values by Sharma et al. [13] and Jewell et al. [14].

The topography of the cells is visualized with an AFM image showing a deepness of 300 nm. This result supports the hypothesis of the scattering of reflected light on the green areas whereas the gold-colored areas are better specular reflectors.

In the near future we will make attempts to analyze smaller spots on the surface of the sample addressing single cells. Complementary imaging polarimetry studies have been initiated and will give valuable information regarding the polarizing properties of the cuticles. The information presented will be used to generate a model of the structure that reproduces the polarizing properties of the exoskeleton of beetles [21].

References

[1] University of Nebraska, Generic Guide to New World Scarab Beetles: http://museum.unl.edu/research/entomology/Guide/Guide-introduction/, Division of Entomology, 2005.
[2] T. Lenau, M. Barfoed, Adv. Eng. Mater. 10 (2008) 299.
[3] A.A. Michelson, Philos. Mag. 21 (1911) 554.
[4] D.H. Goldstein, Appl. Opt. 45 (2006) 7944.
[5] K. Järrendahl, H. Arwin, in: K.J. Eichhorn, K. Hinrichs (Eds.), Ellipsometry of Functional Organic Surfaces and Films, Springer Verlag, 2013.
[6] D.J. Brink, N.G. van der Berg, L.C. Prinsloo, I.J. Hodgkinson, J. Phys. D. Appl. Phys. 40 (2007) 2189.
[7] T.W. Cronin, N. Shashar, R.L. Caldwell, J. Marshall, A.G. Cheroske, T.-H. Chiou, Integr. Comp. Biol. 43 (2003) 549.
[8] P. Brady, M. Cummings, Am. Nat. 175 (2010) 614.
[9] M. Blahó, A. Egri, R. Hegedüs, J. Jósvai, M. Tóth, K. Kertész, L.P. Biró, G. Kriska, G. Horváth, Physiol. Behav. 105 (2012) 1067.
[10] G. Horváth, Naturwissenschaften 95 (2008) 1093.
[11] A. Neville, B. Luke, Tissue Cell 1 (1969) 689.
[12] Y. Bouligand, J. Microsc. 11 (1971) 441.
[13] V. Sharma, M. Crne, J.O. Park, M. Srinivasarao, Science 325 (2009) 449.
[14] S.A. Jewell, P. Vukusic, N.W. Roberts, New J. Phys. 9 (2007) 99.
[15] H. Arwin, R. Magnusson, J. Landin, K. Järrendahl, Philos. Mag. 92 (2012) 1583.
[16] M. Schubert, Phys. Rev. B 53 (1996) 4265.
[17] H. Arwin, T. Berlind, B. Johs, K. Järrendahl, Opt. Express 21 (2013) 22645.

[18] I. Hodgkinson, S. Lowrey, L. Bourke, A. Parker, M.W. McCall, Appl. Opt. 49 (2010) 4558.
[19] H. Arwin, L. Fernández del Río, K. Järrendahl, ICSE-VI, 2013, (this volume).
[20] C. Fallet, PhD Thesis, École Polytechnique, 2011.

[21] J.P. Vigneron, M. Rassart, C. Vandenbem, V. Lousse, O. Deparis, L.P. Biró, D. Dedouaire, A. Cornet, P. Defrance, Phys. Rev. E. 73 (2006) 041905.
[22] A. Parker, R. Townley, E. Helen, Nat. Nanotechnol. 2 (2007) 347.
[23] L. Fernández del Río, Bachelor's thesis, Linköping University, 2011.